Journal of Magnetic Resonance 194 (2008) 222–229

Contents lists available at ScienceDirect

Journal of Magnetic Resonance

journal homepage: www.elsevier.com/locate/jmr

Noise-resilient multi-frequency surface sensor for nuclear quadrupole resonance

A.S. Peshkovsky [a,*], C.J. Cattena [b,1], L.M. Cerioni [b,c], T.M. Osán [b], J.G. Forguez [b], W.J. Peresson [b], D.J. Pusiol [b,c]

[a] RF Sensors, LLC, 701 West 184th Street, Suite 5K, New York, NY 10033, USA
[b] Spinlock Inc., South Dallas, TX, USA
[c] CONICET, Argentina

ARTICLE INFO

Article history:
Received 11 May 2008
Revised 7 July 2008
Available online 10 July 2008

Keywords:
NQR
Radiofrequency coil
RF sensors
Multifrequency coil
Multimodal planar birdcage coil
Nuclear quadrupole resonance
Noise rejection coil
Noise cancellation detector
Sensor with no blind spots, illicit substance detection
Explosives and narcotics detection

ABSTRACT

A planar nuclear quadrupole resonance (NQR) sensor has been developed. The sensor is resilient to environmental noise and is capable of simultaneous independent multi-frequency operation. The device was constructed as an open multimodal birdcage structure, in which the higher modes, generally not used in magnetic resonance, are utilized for NQR detection. These modes have smooth distributions of the amplitudes of the corresponding radiofrequency magnetic fields everywhere along the sensor's surface. The phases of the fields, on the other hand, are cyclically shifted across the sensor's surface. Noise signals coming from distant sources, therefore, induce equal-magnitude cyclically phase-shifted currents in different parts of the sensor. When such cyclically phase-shifted currents arrive at the mode connection point, they destructively interfere with each other and are cancelled out. NQR signals of polycrystalline or disordered substances, however, are efficiently detected by these modes because they are insensitive to the phases of the excitation/detection. No blind spots exist along the sensor's surface. The sensor can be used for simultaneous detection of one or more substances in locations with environmental noise.

1. Introduction

Security technology for controlling the traffic of illicit substances is rapidly growing in demand. Nuclear quadrupole resonance (NQR)-based screening systems have been proven to provide reliable and noninvasive identification of materials containing the so-called quadrupolar nuclei, such as ^{14}N or $^{35,37}Cl$, which are present in most explosives and in many of the narcotics [1]. This methodology is not harmful to individuals or the scanned objects, and permits remote detection without the need for palpation or any mechanical contact. Additionally, automatic operation of the scanners is possible, making this technology much less dependent on the human error.

1.1. Theoretical background

The principles and the instrumentation used in NQR are, generally, similar to those employed in magnetic resonance (MR). There are, however, some important differences between NQR and MR, the most significant of which relates to the manner in which the energy levels are initially established. In MR, the nuclei possessing nonzero magnetic moments become polarized by an externally established static magnetic field, B_0, whose magnitude mainly determines the resonance frequency of the signals coming from the nuclei. In pure NQR, on the other hand, the external magnet is not required because the nuclear levels are established due to coupling between the electric quadrupole moments of nuclei, eQ, and the electric field gradients, eq, internally generated by the charge distributions in the local molecular environments. Nuclei with nonzero electric quadrupole moments (non-spherically symmetrical electric charge distributions) are those with spin $I > 1/2$, which includes such common nuclei as ^{14}N and $^{35,37}Cl$. Although this interaction is purely electric in nature, since the nuclei also possess magnetic dipole moments, it is possible to induce transitions between the nuclear levels with B_1 fields and detect the signals produced by the nuclei in response, much like in MR. Because no external static magnetic field is required, pure NQR spectroscopy is frequently referred to as "MR at zero field".

The Hamiltonian describing the quadrupole interaction in the principal axes frame of the electric field gradient is given in terms of the nuclear spin operators, $\mathbf{I}$, I_x, I_y and I_z, by [2]:

$$H_Q = \frac{e^2Qq}{4I(2I-1)}\left[(3I_z^2 - \mathbf{I}^2) + \eta(I_x^2 - I_y^2)\right] \quad (1)$$

* Corresponding author.
E-mail address: alexey@rf-sensors.com (A.S. Peshkovsky).

[1] Part of this work corresponds to the Physics Degree Thesis of C.J. Cattena presented at Fa.M.A.F, Universidad Nacional de Córdoba, Argentina, 2007.

1090-7807/$ - see front matter © 2008 Elsevier Inc. All rights reserved.
doi:10.1016/j.jmr.2008.07.003

where the quantity e^2Qq is defined as the quadrupole coupling constant of a nucleus in its environment, and η describes the asymmetry of the electric field gradient. The nuclear properties are represented by the quantity eQ and the influence of the electrostatic environment is described by η and eq. For the spin $\mathbf{I} = 1$ ^{14}N nucleus, the three quadrupole eigenstates in terms of eigenstates of the I_z operator, $|1\rangle$, $|0\rangle$ and $|-1\rangle$, are $|+\rangle = (|1\rangle + |-1\rangle)/\sqrt{2}$, $|-\rangle = (|1\rangle - |-1\rangle)/\sqrt{2}$ and $|0\rangle$. The transition frequencies are given by [3]:

$$\upsilon_{\pm} = \frac{e^2Qq}{4h}(3 \pm \eta)$$
$$\upsilon_0 = \upsilon_+ - \upsilon_- = \frac{e^2Qq\eta}{2h} \qquad (2)$$

The NQR spectrum of a compound in which ^{14}N nuclei experience non-axially symmetric electric field gradients ($\eta \neq 0$), therefore, consists of a doublet corresponding to the υ_+ and υ_- transitions and a line at a much lower frequency corresponding to υ_0. The intensity of the transition at υ_+ is at its maximum when the RF field is applied in the *X*-direction of the principal axes frame for the electric field gradient tensor, and the intensity of the υ_- transition is maximized when the B_1 field lies in the *Y*-direction [2,4]. For a powder sample, a B_1 field applied in the laboratory frame is experienced by each crystallite in a different direction in its principal axes frame, with all directions being equally probable.

This leads to an important conclusion: the application of the B_1 field to an isotropic powder sample in every laboratory frame direction appears to produce the same NQR signal in response, although it actually originates from different crystallites in the sample. Since explosives and narcotics are isotropic substances, the direction of the B_1 field used for their identification is, therefore, unimportant. It is important to point out that the situation is different for MR, for which the direction of the B_1 field always has to be orthogonal to the direction of the external static magnetic field.

The frequencies of the NQR measurements are, generally, on the order of several MHz, which is much lower than the frequencies of high-resolution MR. The sensitivity of the measurements is, therefore, also much lower. An important advantage of NQR, however, is in not having to place objects in strong external magnetic fields. This led to a tremendous interest in applying this technology in the field of illicit substance detection, where accurate noninvasive and remote identification of materials is necessary, but the use of the external magnetic fields is undesirable, as it can damage the magnetic parts of the studied objects and endanger people in the vicinity. Additional advantage is that NQR signals exhibit very high specificity to the molecules being observed, thereby providing very reliable material identification, unlike MR, which is more suitable for structure investigations and medical imaging.

1.2. Background on sensor designs with noise rejection properties

Several sensor designs are currently employed in conjunction with NQR scanners. Cylindrical or rectangular RF coils (solenoid, single-turn, multiple loop, etc.) are used for the screening of such objects as luggage or mail, which can be put through the internal volume of the sensors. These coils offer uniform B_1 fields and can be easily shielded from the RF environmental interference by placing an RF shield around the entire sensor (the coil with the screened items contained inside). There are, however, many situations in which it is impossible or undesirable to place the studied objects inside a restricted volume, such as during minefield or human subject scanning. In these cases, surface devices (single turn, spiral, planar solenoid, etc.) are used instead. While these devices offer greater accessibility, they are strongly affected by environmental RF interference coming from distant sources, such as radio stations, computers, switching power supplies, etc.

Reports describing surface sensor designs aimed at introducing environmental interference rejection properties have been made in the past. Garroway et al. [5] and Suits and Garroway [6] reported a gradiometer coil, which is resistant to the environmental noise because it is sensitive only to a spatial derivative of the electromagnetic field. Noise coming from a distant source can be assumed linear in space (wavelengths are much larger than the size of the coil) and, therefore, is not detected. These coils can be made, for example, by forming two electrically connected loops, one above the other, that are wound in the opposite direction. The noise from a distant source induces equal and opposite currents in the loops that cancel each other out. The sample is placed closer to one loop than to the other, and produces a stronger current in one of loop than in the other. It is, therefore, detected by the sensor. A similar idea was subsequently utilized by Smith and Rowe [7] to create a design in which two separate planar solenoid coils were wound in an opposite sense and connected in series or in parallel, or driven by a common circuit that couples them together and to a transmitter or receiver. The coils were positioned one above the other or side by side. Alternatively, the coils were wound in the same sense, but a phase inversion was performed in one of them before the signals from both were combined at the receiver. Noise coming from a distant source was picked up by the two coils and arrived at the receiver as two currents with opposite phases, leading to its self-cancellation. This sensor, therefore, possessed the property of common mode rejection. The sample was always placed closer to one coil than to the other, and its signal was not self-cancelled. While these designs do provide noise cancellation properties, they have an important drawback. The approach of having a dedicated interference detector to be half of the sensor assembly reduces the coil filling factor, ε, by half, which leads to a reduction in signal to noise ratio (SNR), which is proportional to $\sqrt{\varepsilon}$ [8].

Poletto et al. [9] suggested that simultaneous detection of two samples may be realized if each is placed within the active volumes of each of the two coils comprising the sensor assembly similar to the above. They introduced a two-coil detector for the control of forbidden substances hidden in shoes. The coils were constructed such that the distant-source noise signals were attenuated due to their being detected equally by each coil, followed by a phase inversion in one of the coils, leading to self-cancellation upon summation at the receiver. Both coils were involved in sample excitation performed with opposite phases in the two coils. The sample signals were, therefore, also detected with opposite phases, after which one of them underwent a phase inversion, leading to their constructive interference at the receiver. The disadvantage of his approach, however, is that it assumes some prior knowledge of the possible illicit substance location, and provides no detection capability outside of this region (in the region between the coils, for example).

1.3. Background on multi-frequency sensor designs

NQR-active materials normally exhibit multiple resonance lines at a range of frequencies. Simultaneous detection at more than one frequency can be utilized to make the detection very specific, drastically decreasing the possibility of false-positive alarms. Additionally, a sensor with multi-frequency capability could be used for simultaneous detection of various target substances, which is an important practical necessity. The measurements performed with different frequency channels of such sensor need to be independent, and, therefore, the channels have to possess a high degree of isolation (−15 dB is usually sufficient). Common multi-tuned coils, such as surface or solenoid coils, generally rely on the difference in frequencies between the channels as a source of this isola-

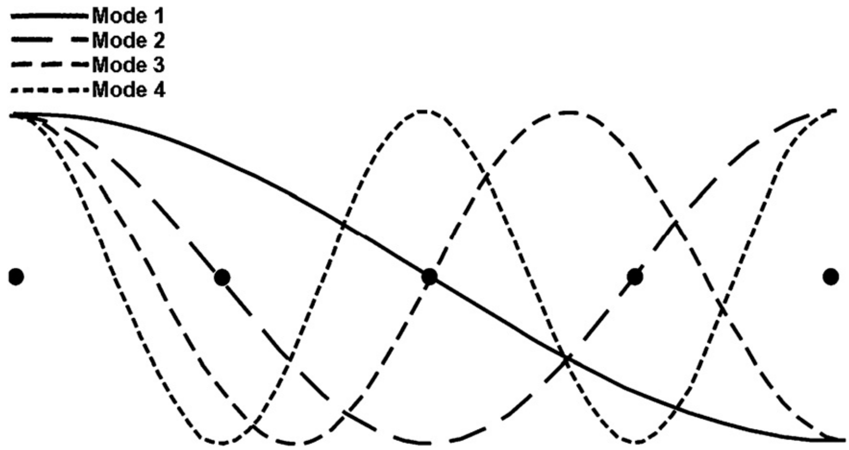

Fig. 1. Current distribution patterns in the legs of the sensor are shown for Mode 1 (surface mode), Mode 2 (butterfly mode), Mode 3 and Mode 4, corresponding to different frequencies of the coil's operation. All modes are orthogonal to each other.

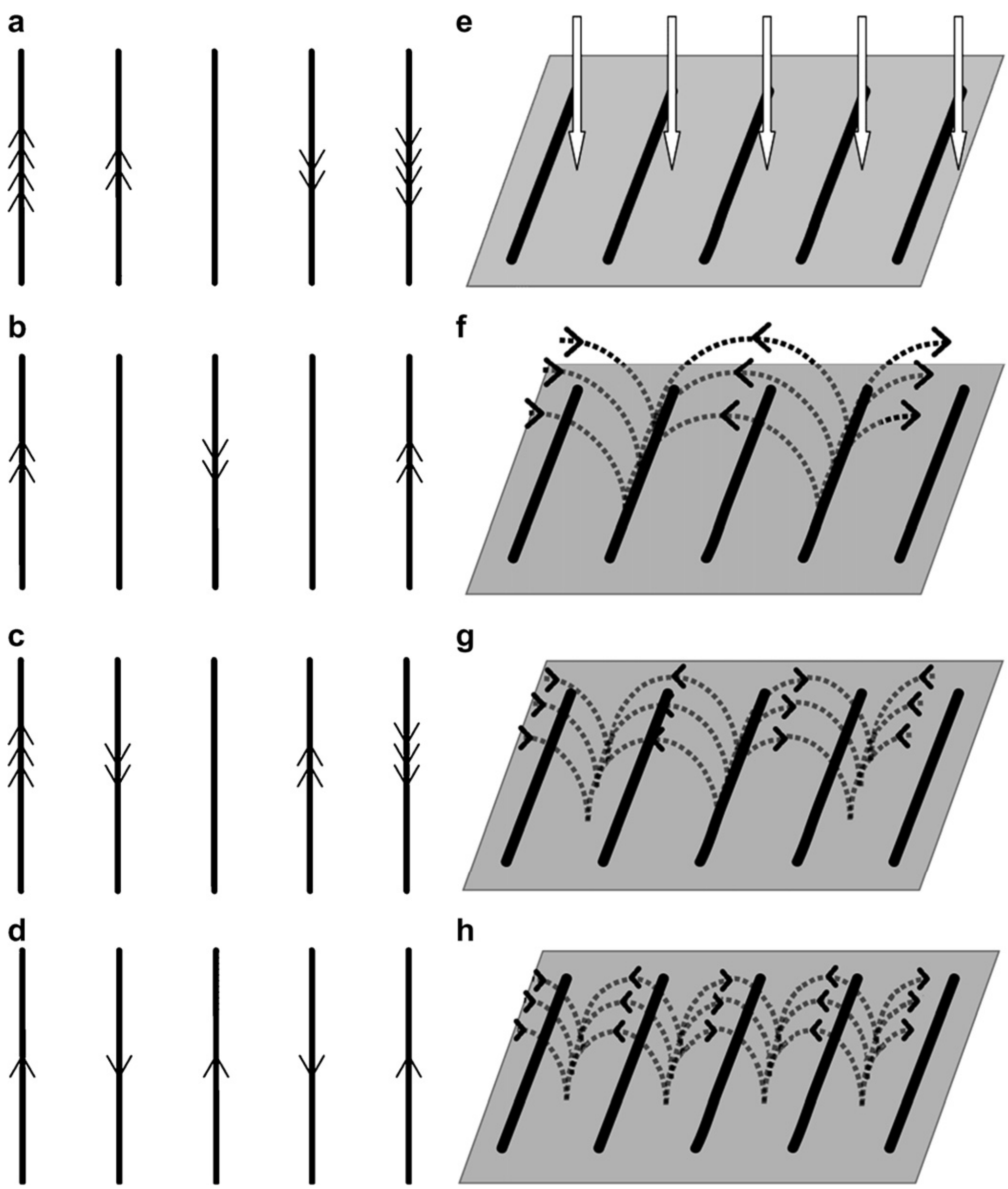

Fig. 2. Schematic view of the current distributions in the legs of the sensor are displayed for all four modes (a – Mode 1, b – Mode 2, c – Mode 3, d – Mode 4), along with the B_1 field patterns occurring due to these currents (e – Mode 1, f – Mode 2, g – Mode 3, h – Mode 4).

tion, and, consequentially, suffer from the inability to have close frequency positioning, which may be required. Lai [10] proposed geometric decoupling to alleviate this issue, utilizing linear surface coils with mutually perpendicular B_1 fields. This approach, however, complicates the shapes of the resulting sensors, restricting accessibility and, therefore, limiting their usefulness. Additionally, only three such universally decoupled cannels are possible, while any additional resonance frequencies are attained by multi-tuning the individual coils, which makes them susceptible to the above-mentioned limitation.

Accordingly, a well designed sensor device for illicit substance detection with NQR should possess the following properties:

1. Noise rejection, such that the signals coming from the scanned objects may be discriminated from the environmental noise.
2. Independence of the prior knowledge of the possible locations of the target substances (sensor without blind spots along its surface).
3. Multi-frequency scanning capability via multiple well isolated channels that can be used at different frequencies simultaneously and independently.
4. Simple shape (planar, for example) that permits easy access for the scanned objects.

In this paper, we introduce a surface sensor that possesses all of the above-mentioned properties. The device is most appropriate for the use in conjunction with a multi-channel NQR spectrometer for the detection of a wide range of illicit substances, such as explosives or narcotics, as well as for any other NQR application, such as industrial process monitoring or quality control.

2. Design principles

The design of the sensor is based on the planar ladder birdcage structure [11–13] that is adapted for NQR-based applications. This structure naturally possesses a number of modes, however, only one or two of these modes are generally used in MR. Higher modes correspond to phase-inhomogeneous RF fields and, therefore, are useless for common MR studies. The sensor design described in this work capitalizes on the potential use of any or all of the other available modes, which, as shown below, possess all the necessary properties, identified in the previous section as desirable for NQR applications.

The sensor described in this work is based on a four-window planar birdcage coil design with five legs carrying the current responsible for the generation and the reception of the B_1 fields in the sensor's working area. A planar birdcage coil can be viewed as a half-wave resonator where a standing wave is formed in the direction perpendicular to the coil's legs. The current amplitudes in the legs are modulated sinusoidally going from one leg to the next, such that an integer number of half-periods fit between the first and the last leg. Modes are formed at different frequencies according to the number of the half-periods. We will refer to the modes by the number of the formed half-periods. It is important to point out that any of the modes may be excited independently from the others, and that it is possible to separately adjust the frequencies of the B_1 fields generated and detected by these modes.

In MR studies, the use of the B_1 fields with uniform magnitudes and phases is preferred. This requirement provides restrictions on the use of the modes available in the multi-modal sensors (only two lowest modes of such sensors are used and their use is, generally, restricted to the central region of the devices). NQR measurements of randomly oriented substances, such as explosives or narcotics, on the other hand, are insensitive to the direction of the B_1 fields, as shown above. Consequentially, any or all of the available modes may be utilized. As shown below, the use of the higher modes provide a number of important advantages.

The current distributions in the legs of the sensor correspond to the naturally formed resonant modes, as shown in Fig. 1. The current flow patterns are shown in more detail in Fig. 2, along with the corresponding B_1 field patterns for each mode. It is evident from Fig. 2e that Mode 1 corresponds to the B_1 field similar to that of a common single-loop surface coil, is relatively uniform in its direction and magnitude, and is oriented perpendicular to the sensor's surface. This mode, which is sometimes called "surface mode", has a high degree of homogeneity and a significant penetration depth. It is, however, susceptible to the common disadvantages of the surface coils, such as a strong affinity to the environmental interference. The B_1 field corresponding to Mode 2, which is sometimes called the "butterfly mode", undergoes one full phase rotation along the sensor's surface, while maintaining a relatively constant magnitude, as illustrated in Fig. 2f. Consequentially, this mode possesses some environmental interference rejection properties, and its penetration depth is not as great as that of Mode 1. The noise arriving in the direction orthogonal to the surface of the coil is sensed by the left and the right sides of the device with

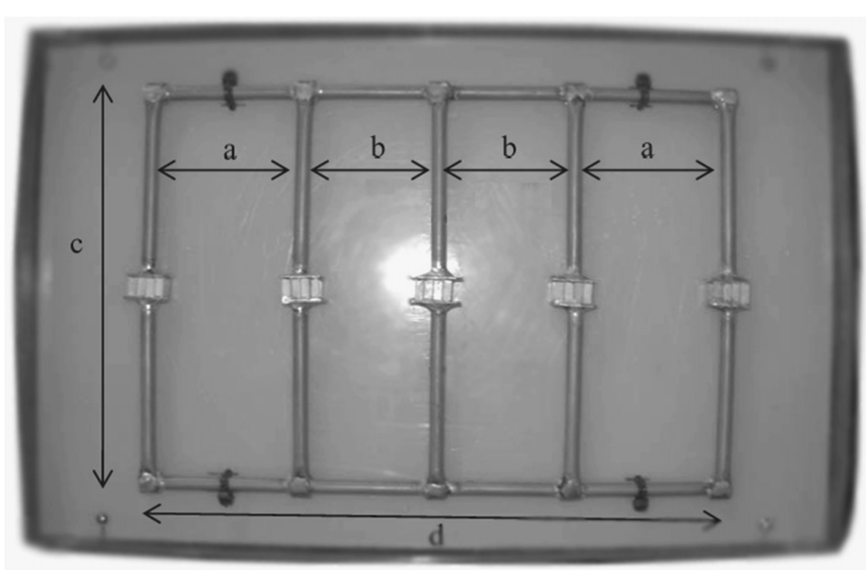

Fig. 3. Photograph of the sensor's active surface is provided, showing the dimensions of the device: a = 6.1 cm, b = 5.1 cm, c = 18.7 cm, d = 25.8 cm.

opposite phases and, therefore, cancels itself out. The situation is, therefore, similar to that described by Pusiol [14], in whose work the noise rejection was achieved by using two separate coils that generated and detected B_1 field in the opposite directions and summed the detected signals at the receiver. The difference is that in the work by Pusiol [14], no field was created or detected in the region of space between the coils, and, therefore, no detection of substances could occur there. Mode 2 of the sensor described in this work possesses the field in its central part as well, where it is oriented parallel to the sensor's surface. This field pattern is similar to the one created by figure-8 or butterfly coil, which has previously been used in MR studies [15]. Detection of the target objects with this mode can, therefore, be made anywhere along the sensor's surface.

For Mode 2 of the sensor described here, as for the sensor described by Pusiol [14] and figure-8 coil [15], the cancellation of the noise arriving from the direction parallel to the coil's surface and orthogonal to its legs depends of the nature of the signal. Homogeneous interference signals coming from distant sources will be better attenuated than those arriving from the nearby sources. This is because the noise rejection properties rely on the fact that the phase of the B_1 field is rotated by one full cycle along the sensor's surface, and if the noise magnitude decreases going from one side of the sensor to the other, cancellation will not be complete. Modes 3 and 4, exemplified in Fig. 2g and h, possess further improved noise rejection properties, since the B_1 fields corresponding to these modes become inverted more than once across the surface area of the sensor. The current distribution in Mode 4 is similar to that created by a meanderline surface coil, which has previously been successfully used for NQR detection of substances [16]. Better rejection of the noise coming from both the distant and the nearby sources is, therefore, obtained. All of the above-mentioned modes are orthogonal to each other and may, therefore, be utilized simultaneously.

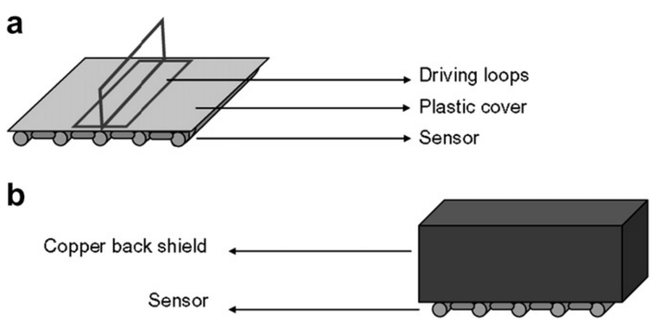

Fig. 4. Sensor driving and back shielding arrangement is presented showing: a – vertical driving loop (coupled to Modes 2 and 4) and horizontal driving loop (coupled to Modes 1 and 3) as well as b – copper shielding box containing the driving loops, placed behind the sensor's active surface.

3. Experimental

Fig. 3 shows a photograph of the active surface of the sensor. The sensor dimensions indicated in the figure were as follows: $a = 6.1$ cm; $b = 5.1$ cm; $c = 18.7$ cm; $d = 25.8$ cm. All conductors were made from copper tubes; each tube was 6.5 mm in diameter. Groups of four 5 nF capacitors (American Technical Ceramics, Huntington Station, NY, USA) were soldered in the middle of each leg of the sensor to provide proper mode frequencies (open low-pass birdcage configuration).

NQR experiments were conducted using Modes 3 and 4. To fine-tune the modes' frequencies the distance between the sensor and its shield (shown in Fig. 4b) was adjusted from the side opposite to the active surface, such that the frequency of Mode 3 arrived at the value of 3.310 MHz. The frequency of Mode 4 was subsequently adjusted to 3.606 MHz by slightly changing capacitor values in the central leg. The latter manipulation did not affect the frequency of Mode 3, which, as shown in Fig. 2c, does not support any current in the central leg and, therefore, is not affected by the present capacitance values.

The driving of the modes was performed by two inductive loops, which were positioned centrally below the sensor's surface orthogonally to each other, as shown in Fig. 4a. The loop driving Mode 3 was parallel to the sensor's surface and the loop driving Mode 4 was orthogonal to it. It can be seen from Fig. 2g and h that this positioning of the loops ensures that the field lines originating from Mode 4 do not cross the plane of the loop used to drive Mode 3 and vice versa. Undesired coupling of the neighboring modes through the driving loops was, therefore, prevented. The figure also makes it clear that Mode 1 could be driven by the loop used to drive Mode 3 and that Mode 2 could be driven by the loop used to drive Mode 4. Better than 15 dB of isolation was achieved between all four modes of the sensor. Each mode had an unloaded Q factor of approximately 200.

To evaluate the noise rejection properties of the different modes of the coil the following experiments were performed:

1. A known low-amplitude signal (−100 dBm) was injected into the receiver at the resonance frequency of each mode (2.092 MHz for Mode 1, 2.885 MHz for Mode 2, 3.310 MHz for Mode 3 and 3.606 MHz for Mode 4) and the receiver's gain was adjusted to compensate for any frequency dependence.

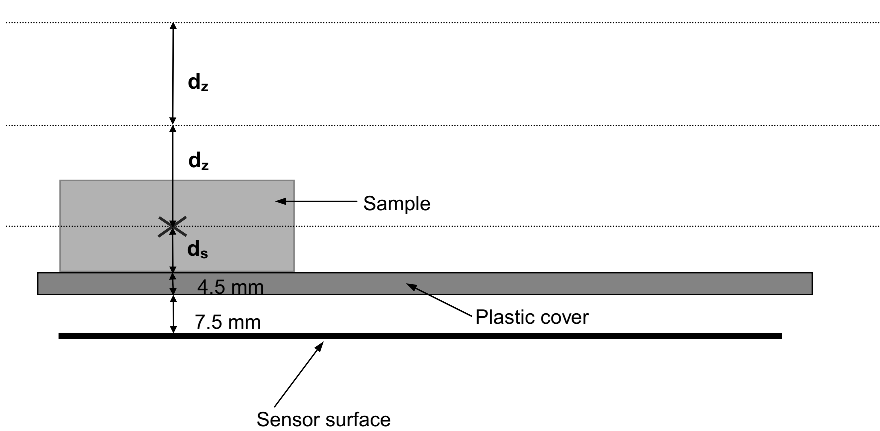

Fig. 5. Experimental setup is shown, where $d_z = 20$ mm and $d_s = 9$ mm for the sample containing $C_6H_{12}N_4$ (detected with Mode 3); $d_z = 10$ mm and $d_s = 12$ mm for the sample containing $NaNO_2$ (detected with Mode 4).

2. White (incoherent) noise was collected and averaged over five measurements for each mode of the coil using the FT spectra in the range between 0 and 15 kHz from the mode frequencies.
3. Coherent noise was generated by placing a transmitting antenna at a distance of 150 cm to the side of the coil, which transmitted a strong interference signal at 10 kHz away from the frequency of each mode. The intensity of the resulting peak in the FT spectra at 10 kHz was averaged over five measurements for each mode of the coil.

Normalized SNR maps for Mode 3 were collected using a sample containing 50 g of hexametilene tetramine ($C_6H_{12}N_4$) at 3.310 MHz, and for Mode 4 using a sample containing 70 g of sodium nitrite ($NaNO_2$) at 3.606 MHz. All the measurements were made at the room temperature. The samples were placed on a 4.5 mm thick plastic cover, which was positioned at three horizontal planes parallel to the sensor surface, as shown in Fig. 5. For the lowest plane, the cover was located at a distance of 7.5 mm above the sensor surface. For the intermediate and the highest planes, the cover was further raised by the distances d_z and $2d_z$, where d_z was 20 mm for $C_6H_{12}N_4$ and 10 mm for $NaNO_2$. The heights of the samples themselves were 18 mm for $C_6H_{12}N_4$ and 20 mm for $NaNO_2$. The distances from the sensor surface to the samples were calculated taking into account the distances from the corresponding planes to the centers of the samples. In order to perform the mappings for each surface, a 24 cm long and 36 cm wide grid was made, consisting of 35 points, distributed every 6 cm. The samples were placed at every point, after which the NQR measurements ware carried out.

Each NQR measurement was conducted using the SSFP pulse sequence with the TONROF method [17]. For measurements involving $C_6H_{12}N_4$, each pulse train consisted of 400 $\pi/2$ pulses separated by $2\tau = 12{,}000\ \mu s$. The receive frequency was shifted by $\Delta f = 24$ kHz from the transmit frequency. For measurements involving $NaNO_2$, each pulse train consisted of 400 $\pi/2$ pulses separated by $2\tau = 1350\ \mu s$. The receive frequency was shifted by $\Delta f = 25$ kHz from the transmit frequency. For each measurement, a four steps phase cycle $(0, \frac{\pi}{2}, \pi, \frac{3\pi}{2})$ was made. The delay between each cycle was 100 ms. The amount of material in each of the samples was selected such that the maximum signal intensity for each sample was similar. Maximum amplitude NQR spectra for both samples are presented in Fig. 6.

In order to measure the noise, identical parameters of the same pulse sequence were used for each mode, and the acquisition was carried out without the samples. The SNR values were determined by the following expression:

$$\mathrm{SNR} = \frac{\text{NQR line amplitude}}{\text{average noise amplitude}} \tag{3}$$

4. Results and discussion

As explained in Section 1.1, the properties of this sensor lead to noise suppression that increases with the increasing mode number. The dependence of the incoherent and coherent types of noise on the mode number is presented in Fig. 7. It can be seen from the figure that both the coherent and the incoherent types of noise are well suppressed by Modes 2–4 of the coil and that Mode 4 is capable of attenuating both types of noise by a factor of over 10 compared to Mode 1, and, therefore, compared with the common surface coils.

The SNR maps collected using Mode 3 (with $C_6H_{12}N_4$ at 3.310 MHz) are presented in Fig. 8a–c; the SNR maps collected using Mode 4 (with $NaNO_2$ at 3.606 MHz) are presented in Fig. 8d–f. The maps correspond to the predicted current and field patterns for the modes, shown in Fig. 2. Mode 3 supports no current in the central leg, which led to a slight field strength reduction at that location. Correspondingly, the SNR maps for Mode 3 show

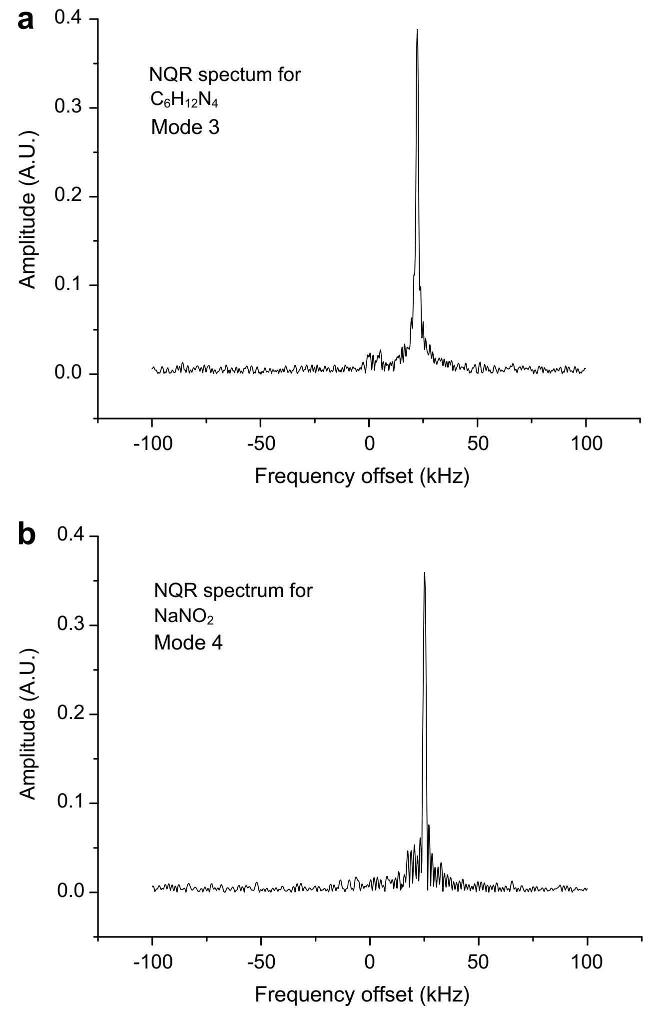

Fig. 6. Maximum amplitude NQR spectra for $C_6H_{12}N_4$ (detected with Mode 3) and $NaNO_2$ (detected with Mode 4) are presented.

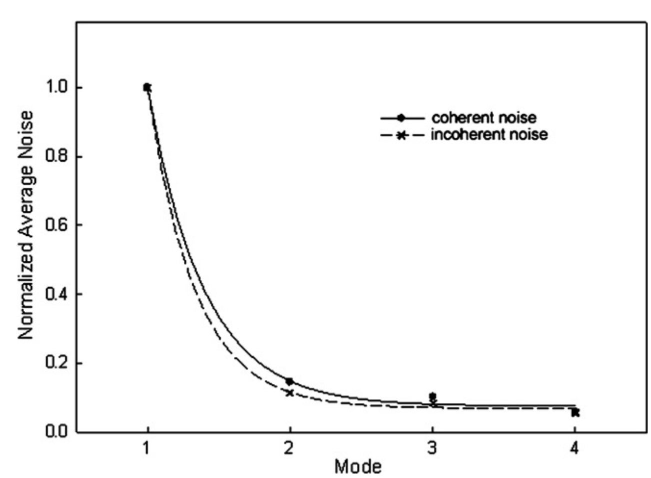

Fig. 7. The dependence of the normalized averaged coherent and incoherent noise intensities on the mode number is presented, showing an increasing ability of the higher modes to reject both types of the noise.

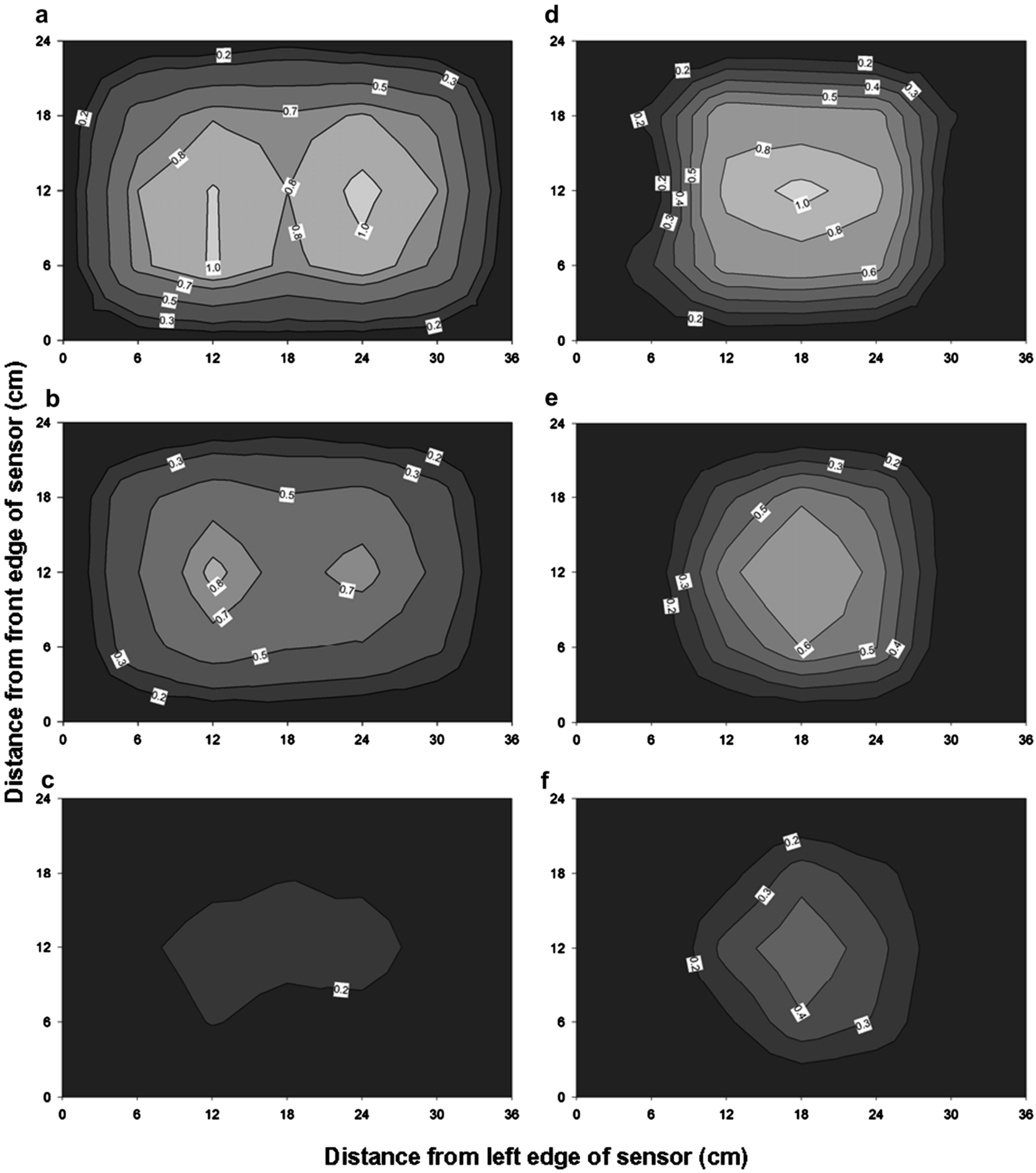

Fig. 8. SNR maps collected using Mode 3 (with $C_6H_{12}N_4$ at 3.310 MHz) are presented on the left-hand side for a range of distances between the sample and the sensor's surface: a – 21 mm, b – 41 mm, c – 61 mm. SNR maps collected using Mode 4 (with $NaNO_2$ at 3.606 MHz) are presented on the right-hand side for a range of distances between the sample and the sensor's surface: d – 24 mm, e – 34 mm, f – 44 mm.

noticeable intensity reductions in the central region. This feature was largely compensated by reducing the separation between the adjacent legs of the coil, as shown in Fig. 3 (dimension b is somewhat smaller than dimension a). Mode 4, on the other hand, did not display such feature, as expected from its current and field pattern.

The usefulness of the sensor can be evaluated based on the SNR maps provided in Fig. 8 and on the profiles taken horizontally through the centers of the maps, displayed in Fig. 9. It can be estimated from this data that reliable detection of substances containing less than 100 g of the NQR active materials can be performed by this sensor in few seconds up to the sample distances of about

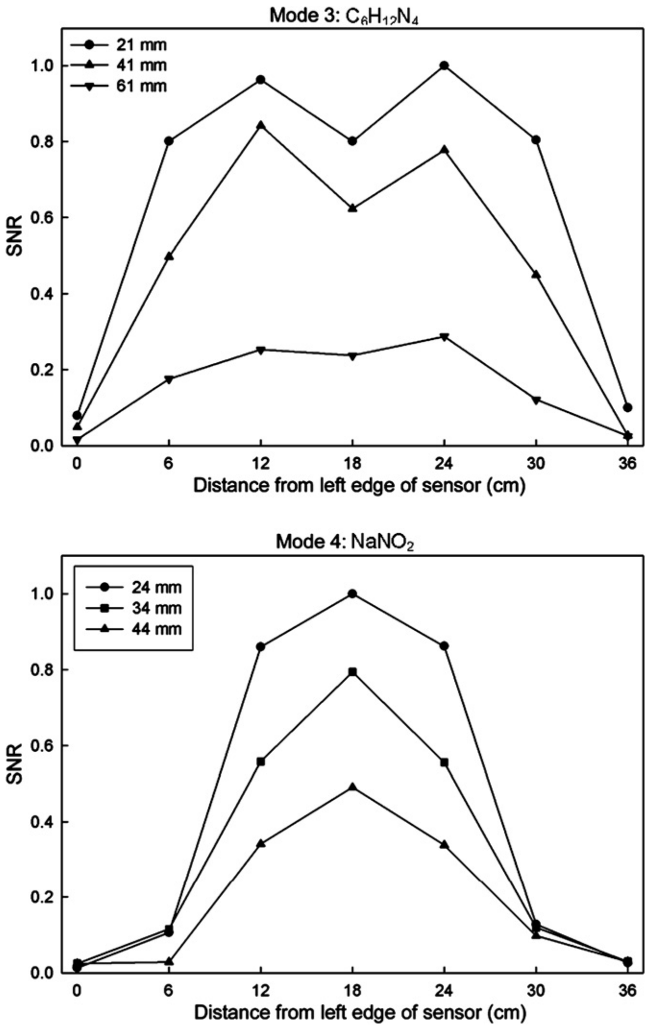

Fig. 9. Horizontal profiles taken through the centers of the SNR maps displayed in Fig. 8 are presented. Estimations of the active volumes corresponding to Mode 3 and Mode 4 can be made from the SNR maps and these profiles.

6 cm for Mode 3 and about 5 cm for Mode 4 of this sensor. These distances are sufficient for many applications, such as the detection of illicit substances hidden on a human body. The size of the sensor used in this study was, however, chosen based only on convenience of the evaluation work. In situations where greater active distances are required, larger size sensors should be used. Slightly lower active distances were expected for Mode 4 based on its field profile, which is confirmed by this study. On the other hand, this mode is capable of a larger degree of noise rejection, which is also confirmed by the presented data. Since the modes are completely independent, they can potentially be jointly used for the simultaneous detection of two substances.

5. Conclusions

We have successfully designed and constructed a planar surface sensor device suitable for illicit substance detection with NQR. The sensor has no blind spots, is capable of the environmental noise rejection and can be used for simultaneous multi-frequency scanning via multiple well isolated channels. The noise rejection properties of the sensor were evaluated for four of its independent channels (modes). The performance of the device was evaluated using sample substances at two different frequencies using two independent sensor channels (modes). All experimental results corresponded to the theoretical predictions provided in this paper. This device could be used for the detection of a wide range of illicit substances, such as explosives or narcotics, as well as for any other NQR application, such as industrial process monitoring or quality control.

References

[1] A.N. Garroway, M.L. Buess, J.B. Miller, B.H. Suits, A.D. Hibbs, G.A. Barrall, R. Matthews, L.J. Burnett, Remote sensing by nuclear quadrupole resonance, IEEE Trans. Geosci. Remote Sensing 39 (2001) 1108–1118.

[2] C.P. Slichter, Principles of Magnetic Resonance, third ed., Springer, Berlin, 1990.

[3] J.P. Yesinowski, M.L. Buess, A.N. Garroway, M. Ziegeweid, A. Pines, Detection of ^{14}N and $_{35}$Cl in cocaine base and hydrochloride using NQR, NMR, and SQUID techniques, Anal. Chem. 67 (1995) 2256–2263.

[4] J.B. Miller, B.H. Suits, A.N. Garroway, Circularly polarized RF magnetic fields for spin-1 NQR, J. Mag. Reson. 151 (2001) 228–234.

[5] B.H. Suits, A.N. Garroway, J.B. Miller, Noise-immune coil for unshielded magnetic resonance measurements, J. Mag. Reson. 131 (1998) 154–158.

[6] B.H. Suits, A.N. Garroway, Radiofrequency surface detection coil, US Patent 6924644, 2005.

[7] J.A. Smith, M.D. Rowe, Apparatus for and method of nuclear quadrupole resonance testing a sample, US Patent 6486838, 2002.

[8] C.P.J. Poole, Electron Spin Resonance: A Comprehensive Treatise on Experimental Techniques, Wiley, New York, 1983.

[9] G.E. Poletto, T.M. Osan, D.J. Pusiol, Pulsed ^{14}N NQR device designed to detect substances in the presence of environmental noise, Hyperfine Interact. 159 (2004) 127–130.

[10] C.M. Lai, Wideband NQR system using multiple de-coupled RF coils, US Patent 6822444, 2004.

[11] J. Jin, Electromagnetic Analysis and Design in Magnetic Resonance Imaging, CRC Press, Boca Raton, FL, 1999.

[12] C.H. Oh, S.K. Kim, Y.J. Yang, C.B. Ahn, Novel Type of quadrature breast RF coil with a ladder structure, in: Proceedings of the ISMRM, 6th Meething, Sydney, Australia, 1998, p. 2025.

[13] H. Fujita, W.O. Braum, S.M. Shvartsman, R.W. Brown, T.J. Reisker, D.A. Molyneaux, M.A. Morich, An optimized open quadrature distributed RF surface coil, in: Proceedings of the ISMRM, 6th Meething, Sydney, Australia, 1998, p. 645.

[14] D.J. Pusiol, Sensor assembly and method for the detection of substances by nuclear quadrupolar resonance (NQR) and in presence of environmental interference, US Patent 7292033, 2007.

[15] B. Blumich, V. Anferov, S. Anferova, M. Klein, R. Fechete, An NMR-MOUSE for analysis of thin objects, Macromol. Mater. Eng. 288 (2003) 312–317.

[16] M.L. Buess, A.N. Garroway, J.B. Miller, NQR detection using a meanderline surface coil, J. Mag. Reson. 92 (1991) 348–362.

[17] L.M.C. Cerioni, D.J. Pusiol, A new method to obtain frequency offsets in NQR multi-pulse sequences, Hyperfine Interact. 159 (2004) 389–393.